

Communication

# Effects of zero-filling and apodization on spectral integrals in discrete Fourier-transform spectroscopy of noisy data

Andreas Ebel<sup>a,b,\*</sup>, Wolfgang Dreher<sup>c,d</sup>, Dieter Leibfritz<sup>c,d</sup>

<sup>a</sup> Department of Radiology, University of California San Francisco, DVA Medical Center San Francisco, MR Unit (114M), 4150 Clement St., San Francisco, CA 94121, USA

<sup>b</sup> Northern California Institute for Research and Education, DVA Medical Center San Francisco, MR Unit (114M), 4150 Clement St., San Francisco, CA 94121, USA

<sup>c</sup> Universität Bremen, Fachbereich 2 (Chemie), Leobener Str., 28334 Bremen, Germany

<sup>d</sup> Center of Advanced Imaging (CAI), 28359 Bremen, Germany

Received 15 March 2006; revised 12 June 2006

Available online 17 July 2006

## Abstract

The influence of noise on the standard deviation of spectral integrals is examined. Calculations assuming discrete Fourier-transform data are compared with Monte-Carlo simulations. The effects of zero-filling and apodization are examined for free-induction-decay (FID) signals and for symmetric spin-echo signals in one and two dimensions, with particular attention to features not previously presented in the literature. Findings suggest that for mild apodization, the known sensitivity enhancement due to zero-filling in either the real or the imaginary part signal [E. Bartholdi, R.R. Ernst, Fourier spectroscopy and the causality principle, *J. Magn. Reson.*, 11 (1973) 9–19] is maintained; however, for stronger apodization filters, this enhancement can be obliterated completely. It is shown that results obtained by analysis of one-dimensional signals can be readily applied to multi-dimensional data. Furthermore, zero-filling has a negligible effect for symmetric spin-echo signals with implications for signal averaging in magnetic resonance imaging and spectroscopic imaging.

© 2006 Elsevier Inc. All rights reserved.

**Keywords:** Fourier transform; Spectral integration; Zero-filling; Apodization; NMR spectroscopy

## 1. Introduction

It is well known that the extension of a discretely sampled time-domain signal by zeroes (zero-filling) to twice the number of data points is equivalent to an interpolation process, which increases the information content of either absorption or dispersion mode signal by the amount of additional information contained in the other signal [1]. This also doubles the signal energy, and hence increases the maximum signal-to-noise ratio (SNR) by a factor of  $\sqrt{2}$  [1]. At the same time, zero-filling can be interpreted as a means of increasing effective spectral resolution [2]. Zero-filling beyond twice the number of original data points only leads to a trigonometric

interpolation, which provides no further SNR enhancement [1], and allows resolution enhancement only in rare cases [2]. Another widely used procedure for sensitivity enhancement is apodization, i.e., the multiplication of the time-domain signal with a window function that typically attenuates the parts of the signal that exhibit low SNR [2]. Both, zero-filling and apodization significantly impact the influence of noise on results of direct summation of spectral points (spectral integration) in Fourier-transformed data. In spite of the fact that frequency-domain and time-domain fitting procedures for spectral quantification have gained in popularity in recent years, spectral integration is still widely used.<sup>1</sup>

<sup>1</sup> The terms time-domain and frequency-domain are chosen because of their relevance to NMR spectroscopy. In the general case of Fourier-transform reconstruction applied to discretely sampled data, they can be replaced by acquisition domain and reconstruction domain, respectively.

\* Corresponding author. Fax: +1 415 668 2864.  
E-mail address: [andreas.ebel@ucsf.edu](mailto:andreas.ebel@ucsf.edu) (A. Ebel).

Examples include high-resolution NMR spectroscopy [3], *in vivo* <sup>13</sup>C NMR spectroscopy [4], *in vivo* <sup>1</sup>H NMR spectroscopy [5,6], as well as *in vivo* 2D <sup>1</sup>H NMR spectroscopy [7]. Furthermore, the widely used averaging of voxel intensities in magnetic resonance spectroscopic imaging (MRSI) or magnetic resonance imaging (MRI) needs to be included if Fourier-transform reconstruction is applied for image formation. The drawbacks of the direct summation approach, including systematic errors [8–12] and random errors [8,10,13–15], have been discussed to some extent in the literature. However, in most studies of random errors, NMR data was treated as continuous [8,10,13,14]. Even though, this approach has certain advantages, it fails to take into account the effects of zero-filling. While in the work by Bourg and Nuzillard [15] the discrete nature of the NMR data was appreciated, several aspects of the influence of noise on peak integrals obtained by direct summation were neglected. In this communication, recognizing the absence of a thorough analysis of the effects of zero-filling and apodization on the standard deviation of spectral integrals for discretely sampled free-induction decay (FID) and spin-echo signals in one and multiple dimensions, errors in spectral integrals due to random noise will be discussed. The importance of zero-filling in combination with apodization, and, for symmetric spin-echo signals, temporal shifting of the signal will be discussed in the context of 1D and 2D NMR spectroscopy, as well as MRSI. The theoretical analysis of the signal properties will be validated with Monte-Carlo simulations. This treatment is based in part on our earlier work [16].

## 2. Theory

In the following, a discrete, one-dimensional time-domain signal will be considered, consisting of  $N$  uncorrelated, complex noise values (additive Gaussian white noise),  $w_n$  ( $n = 0, \dots, N - 1$ ), with zero mean and standard deviation  $\sigma_t$ . The standard deviation of the spectral integral obtained by direct summation over  $I'$  points after zero-filling, apodization and an optional shift of the time-domain signal prior to Fourier transform (FT) will be calculated. The shift by  $M$  points ( $0 \leq M < N$ ) is needed in case of spin-echo signals in order to place the point corresponding to the echo time, i.e.,  $t = 0$ , at the start of the signal array. A sampling interval of  $\Delta t = 1$  is assumed corresponding to a spectral resolution of  $1/N$ . After FT, the spectral noise is given by

$$W_\ell = \sum_{n=0}^{N'-1} w'_n a_n \exp(-2\pi i n \ell / N'), \quad (1)$$

where  $i$  is the imaginary unit,  $\ell = -N'/2, \dots, (N'/2) - 1$ , and the coefficients  $a_n$  represent the values of a time-domain apodization function. With zero-filling from  $N$  to  $N'$  points

$$w'_n = \begin{cases} w_n & \text{for } 0 \leq n < N \leq N' \\ 0 & \text{otherwise.} \end{cases} \quad (2)$$

Applying the time shift by  $M$  points to the left,

$$w'_n = \begin{cases} w_{n+M} & \text{for } 0 \leq n < N - M \\ 0 & \text{for } N - M \leq n < N' - M \\ w_{n+M-N'} & \text{for } N' - M \leq n < N'. \end{cases} \quad (3)$$

Taking the sum in Eq. (1) over these three index ranges, a suitable conversion of summation indices can be used and the result summarized as follows:

$$W_\ell = \exp(2\pi i M \ell / N') \cdot \sum_{n=0}^{N-1} w_n a_n \exp(-2\pi i n \ell / N'). \quad (4)$$

This reflects, of course, the well-known fact that the shift of the time-domain signal corresponds to a phase rotation in the spectrum. Since the FT represents a weighted sum of the values of the time-domain signal, the mean of the spectral noise,  $W_\ell$ , remains zero. Note that for a FID signal, the shift parameter  $M$  is 0, and the signal value at the first time point is multiplied by 1/2. This multiplication accounts for the fact that only non-negative sampling times are considered, and consequently only half of the first sampling interval centered at  $t = 0$  falls into the acquisition window [17]. It can be shown that if the entire spectrum is summed (integrated), the standard deviation of the result is  $\sigma_{N'} = \sigma_t$  for a spin-echo-type signal, regardless of zero-filling and shift of the time-domain signal, or  $\sigma_{N'} = \sigma_t/2$  for an FID signal, regardless of zero-filling. This is in agreement with the fact that in this case, the integral value is identical with the value of the time-domain signal at time  $t = 0$ . Note that for the purposes of this communication, the standard deviation of the complex-valued spectral integral is represented by the standard deviation of the real part, which is identical to that of the imaginary part. If, in general, the  $I'$  spectral points of the interval  $[\ell_1, \dots, \ell_2]$ , with  $\ell_2 = \ell_1 + I' - 1$  and  $1 < I' \leq N'$ , are integrated, the variance of the resulting integral<sup>2</sup>

$$\mathfrak{V} := \frac{1}{N'} \sum_{\ell=\ell_1}^{\ell_2} W_\ell \quad (5)$$

is given by

$$\begin{aligned} V(\mathfrak{V}) &= E(|\mathfrak{V}|^2) \\ &= \frac{1}{N'^2} \sum_{n,m=\ell_1}^{\ell_2} E(W_n W_m^*) \\ &= \frac{1}{N'^2} \sum_{n,m} E \left\{ \exp(+2\pi i M n / N') \sum_{j=0}^{N-1} w_j a_j \exp(-2\pi i j n / N') \right. \\ &\quad \left. \times \exp(-2\pi i M m / N') \sum_{p=0}^{N-1} w_p^* a_p \exp(+2\pi i p m / N') \right\} \\ &= \frac{1}{N'^2} \sum_{n,m} \sum_{j,p} E(w_j w_p^*) a_j a_p \exp[-2\pi i ((j - M)n - (p - M)m) / N']. \end{aligned}$$

<sup>2</sup> The factor  $1/N'$  represents the spectral resolution,  $\Delta v : \mathfrak{V} = \int_{v_1}^{v_2} W(v) dv \approx \sum_{\ell=\ell_1}^{\ell_2} W_\ell \cdot \Delta v = \frac{1}{N'} \sum_{\ell=\ell_1}^{\ell_2} W_\ell$ .

Here, Eq. (4) was used, and the asterisk denotes complex conjugation. Since  $w_j$  and  $w_p^*$  are uncorrelated, only the terms with  $j = p$  remain

$$V(\mathfrak{I}) = \frac{1}{N'^2} \sum_{n,m} \sum_{j=0}^{N-1} E(|w_j|^2) a_j^2 \exp[-2\pi i(j-M)(n-m)/N']. \quad (6)$$

In the derivation leading to Eq. (6), the expression  $\sum_{n,m=\ell_1}^{\ell_2} E(W_n W_m^*)$  represents the sum of covariances between all pairs of spectral points within the integration interval. Therefore, the variance of the integral  $\mathfrak{I}$  represents a measure of correlation among the spectral points integrated [18].

The expectation value in Eq. (6) is the variance of the complex-valued time-domain noise and equals  $2\sigma_t^2$  for spin-echo-type signals for all  $j$  and for FID signals for  $j \neq 0$ , and  $\sigma_t^2/2$  for FID signals for  $j = 0$ . As mentioned earlier, the standard deviation of the real and the imaginary part of  $\mathfrak{I}$  is given by  $\sigma_{N'}(I') = \sqrt{V(\mathfrak{I})/2}$ , which will be written as

$$\sigma_{N'}(I') = \sigma_t \frac{\sqrt{X}}{N'}. \quad (7)$$

The quantity  $X$  is defined as

$$X_{SE} := \sum_{n,m=\ell_1}^{\ell_2} \sum_{j=0}^{N-1} a_j^2 \exp[-2\pi i(j-M)(n-m)/N'], \quad (8a)$$

for spin-echo-type signals, and as

$$X_{FID} := \sum_{n,m=\ell_1}^{\ell_2} \left\{ \sum_{j=1}^{N-1} a_j^2 \exp[-2\pi i j(n-m)/N'] + \frac{1}{4} \right\} \quad (8b)$$

for FID signals. Here and in the following, equations with a label “a” apply to spin-echo signals, while those with a label “b” apply to FID signals. In Eq. (8b), it is assumed that  $a_0 \equiv 1$  for any apodization filter. Note that it follows from the form of Eq. (7) that if the spectral noise within the integration interval is uncorrelated, the quantity  $X$  is proportional to the number of integrated points,  $I'$ , corresponding to incoherent averaging of noise [19,20].

The expressions for  $X$  given in Eqs. (8a) and (8b) can be simplified as follows:

$$X_{SE} = \sum_{j=0}^{N-1} a_j^2 \sum_{n>m} \{ \exp[-2\pi i(j-M)(n-m)/N'] + \exp[+2\pi i(j-M)(n-m)/N'] \} + I' \sum_{j=0}^{N-1} a_j^2, \quad (9a)$$

and

$$X_{FID} = \sum_{j=1}^{N-1} a_j^2 \sum_{n>m} \{ \exp[-2\pi i j(n-m)/N'] + \exp[+2\pi i j(n-m)/N'] \} + I' \sum_{j=1}^{N-1} a_j^2 + \frac{1}{4} I'^2, \quad (9b)$$

where the last term in Eq. (9a) and the last two terms in Eq. (9b) result from the summation of all terms with  $n = m$ . Each difference  $d := n - m$ , with  $d \in [1, \dots, I' - 1]$ , for

$n > m$ , is present  $(I' - d)$  times. Therefore, using  $A := \sum_{j=0}^{N-1} a_j^2$ :

$$X_{SE} = \sum_{j=0}^{N-1} a_j^2 \sum_{d=1}^{I'-1} \{ (I' - d) [\exp[-2\pi i(j-M)d/N'] + \exp[+2\pi i(j-M)d/N']] \} + AI', \quad (10a)$$

and

$$X_{FID} = \sum_{j=1}^{N-1} a_j^2 \sum_{d=1}^{I'-1} \{ (I' - d) [\exp[-2\pi i j d/N'] + \exp[+2\pi i j d/N']] \} + I'(A - 1) + \frac{1}{4} I'^2. \quad (10b)$$

With the definition  $q_{\pm} := \exp(\pm 2\pi i d/N')$ , Eqs. (10a) and (10b) become

$$X_{SE} = AI' + \sum_d \left[ (I' - d) \sum_{j=0}^{N-1} a_j^2 (q_-^{j-M} + q_+^{j-M}) \right], \quad (11a)$$

and

$$X_{FID} = I'(A - 1) + \frac{1}{4} I'^2 + \sum_d \left[ (I' - d) \sum_{j=1}^{N-1} a_j^2 (q_-^j + q_+^j) \right]. \quad (11b)$$

In the following, three cases will be considered: (i) general apodization; (ii) exponential apodization; and (iii) no apodization.

### 2.1. General apodization

In the inner sum of Eqs. (11a) and (11b), the identity  $q_-^k + q_+^k = 2 \cdot \cos[2\pi dk/N']$  can be used, where  $k$  is either  $j - M$  (Eq. (11a)) or  $j$  (Eq. (11b)):

$$X_{SE} = AI' + 2 \sum_d \left\{ (I' - d) \sum_{j=0}^{N-1} a_j^2 \cos[2\pi d(j-M)/N'] \right\}, \quad (12a)$$

and

$$X_{FID} = I'(A - 1) + \frac{1}{4} I'^2 + 2 \sum_d \left\{ (I' - d) \sum_{j=1}^{N-1} a_j^2 \cos[2\pi d j/N'] \right\}. \quad (12b)$$

However, in general, the presence of the apodization coefficients will not allow further simplification.

### 2.2. Exponential apodization

The apodization coefficients  $a_j = \exp(-\alpha \pi j \Delta t)$ , with line broadening  $\alpha$  and sampling interval  $\Delta t$  in the time-domain, can be incorporated into the expressions for  $q_{\pm}$  allowing evaluation of the geometrical sums:

$$B_{SE\pm}(d) := \sum_{j=0}^{N-1} \exp[-2\alpha \pi j \Delta t \pm 2\pi i d(j-M)/N'] = \exp(\mp 2\pi i d M/N') \frac{1 - \exp(-2\alpha \pi N \Delta t \pm 2\pi i d N/N')}{1 - \exp(-2\alpha \pi \Delta t \pm 2\pi i d/N')}, \quad (13a)$$

and

$$B_{\text{FID}\pm}(d) := \sum_{j=1}^{N-1} \exp[-2\alpha\pi j\Delta t \pm 2\pi idj/N']$$

$$= \frac{1 - \exp(-2\alpha\pi N\Delta t \pm 2\pi idN/N')}{1 - \exp(-2\alpha\pi\Delta t \pm 2\pi id/N')} - 1. \quad (13b)$$

Similarly, the geometric sum defining  $A = \sum_{j=0}^{N-1} \exp(-2\alpha\pi j\Delta t)$  can be evaluated leading to

$$A = \sum_{j=0}^{N-1} \exp(-2\alpha\pi j\Delta t) = \frac{1 - \exp(-2\alpha\pi N\Delta t)}{1 - \exp(-2\alpha\pi\Delta t)}. \quad (14)$$

Thus, only a single sum remains to be evaluated in the expression for  $X$ , and Eqs. (11a) and (11b) become

$$X_{\text{SE}} = I' \frac{1 - \exp(-2\alpha\pi N\Delta t)}{1 - \exp(-2\alpha\pi\Delta t)}$$

$$+ \sum_{d=1}^{I'-1} \{(I' - d)[B_{\text{SE}+}(d) + B_{\text{SE}-}(d)]\}, \quad (15a)$$

and

$$X_{\text{FID}} = I' \left( \frac{1 - \exp(-2\alpha\pi N\Delta t)}{1 - \exp(-2\alpha\pi\Delta t)} - 1 \right)$$

$$+ \frac{1}{4} I'^2 + \sum_{d=1}^{I'-1} [(I' - d)(B_{\text{FID}+}(d) + B_{\text{FID}-}(d))]. \quad (15b)$$

### 2.3. No apodization

With all  $a_j = 1$ , the inner sum in Eqs. (11a) and (11b) can be evaluated as a geometric sum (see Appendix A) and rewritten as

$$X_{\text{SE}} = NI'$$

$$+ \sum_{d=1}^{I'-1} \left\{ (I' - d) \frac{\sin[\pi d(1 + 2M)/N'] + \sin[2\pi d(N - \frac{1}{2} - M)/N']}{\sin(\pi d/N')} \right\}, \quad (16a)$$

and

$$X_{\text{FID}} = I' \left( N - \frac{1}{4} I' - \frac{1}{2} \right)$$

$$+ \sum_{d=1}^{I'-1} \left\{ (I' - d) \frac{\sin[2\pi d(N - \frac{1}{2})/N']}{\sin(\pi d/N')} \right\}. \quad (16b)$$

In the absence of zero-filling ( $I' = I$ ,  $N' = N$ ), it is straightforward to show [16] that

$$\sigma_N(I) = \sigma_t \frac{\sqrt{X}}{N} = \begin{cases} \sigma_t \sqrt{\frac{I}{N}} & \text{for spin-echo signals and} \\ \sigma_t \sqrt{\frac{I}{N} - \frac{3I^2}{4N^2}} & \text{for FID signals.} \end{cases} \quad (17a)$$

$$(17b)$$

Note that  $I/I' = N/N'$ . The result for spin-echo signals reflects the incoherent addition of uncorrelated spectral noise. It furthermore shows again that if the entire spectrum were to be integrated, i.e.,  $I = N$ ,  $\sigma_N = \sigma_t$  for spin-echo signals, and  $\sigma_N = \sigma_t/2$  for FID signals. Note that

for FID signals, the multiplication of the first point by 1/2 introduces a correlation of the spectral noise as demonstrated by the deviation of  $\sigma_N(I)$  in Eq. (17b) from the proportionality  $\sigma_N(I) \propto \sqrt{I}$  expected for uncorrelated spectral noise [19,20]. In fact, it can be shown that, without this multiplication, the spectral noise remains uncorrelated [16].

In addition, for FID signals, the result for zero-filling with  $N' = 2N$  can be derived analytically (see Appendix B) to be

$$X_{\text{FID}} = 2I \left( N - \frac{1}{2} I - \frac{1}{2} \right) + I = 2I \left( N - \frac{1}{2} I \right), \quad (18)$$

and therefore

$$\sigma_{2N}(I) = \sigma_t \sqrt{\frac{I}{2N} - \frac{I^2}{4N^2}}. \quad (19)$$

Here, the quantities  $I'$  and  $N'$  are, respectively, expressed in terms of the interval size and number of data points in the spectrum obtained without zero-filling. Again, the deviation of  $\sigma_{2N}(I)$  from the proportionality  $\sigma_{2N}(I) \propto \sqrt{I}$  indicates a correlation among the spectral noise within the integration interval. In fact, it can be shown that, even without the multiplication of the first point by 1/2, zero-filling causes a correlation among spectral points [16].

### 3. Results

In Figs. 1–4 are shown results of Monte-Carlo simulations (symbols) in comparison to predictions (lines) based on the theory outlined in the previous section (see caption of Fig. 1 for more details on the simulations). In particular, Fig. 1 shows the standard deviation of integrated noise,  $\sigma_{N'}$ , in units of the standard deviation of noise in the FID signal,  $\sigma_t$ , plotted against the integrated fraction of the spectrum,  $I'/N'$ . Good agreement between the predicted values and the simulation results is obtained for (i) no zero-filling, (ii) zero-filling only, and (iii) zero-filling and exponential apodization. Fig. 2 shows  $\sigma_{N'}/\sigma_t$ , plotted against the number of spectral points after zero-filling,  $N'$ , in units of  $N$ . The theoretical predictions match the simulated data well for all values of exponential line broadening applied. Fig. 3 shows the ratio of the standard deviation of integrated noise based on an FID signal processed without zero-filling,  $\sigma_N$ , versus with zero-filling,  $\sigma_{2N}$ , plotted against the strength of the apodization filter. For both, exponential and Gaussian filters, good agreement between simulations and theory can be observed. Note that without apodization and for the small integration interval considered in Fig. 3,  $\sigma_N/\sigma_{2N}$  approaches the value of  $\sqrt{2}$  in agreement with Eqs. (17b) and (19) for the limiting case  $I \ll N$ . The effect of the time shift, by  $M$  points, prior to FT is demonstrated in Fig. 4, which shows  $\sigma_{N'}/\sigma_t$  versus  $N'/N$ . For both cases,  $M = 0$  and  $M = N/2$ , good agreement between simulated data and prediction is observed.

In Fig. 5 is shown the ratio of the standard deviation of integrated noise,  $\sigma_{N',N'}(I',J')$ , with zero-filling  $N' = 2N$  versus  $N' = N$  according to a two-dimensional Monte-Carlo

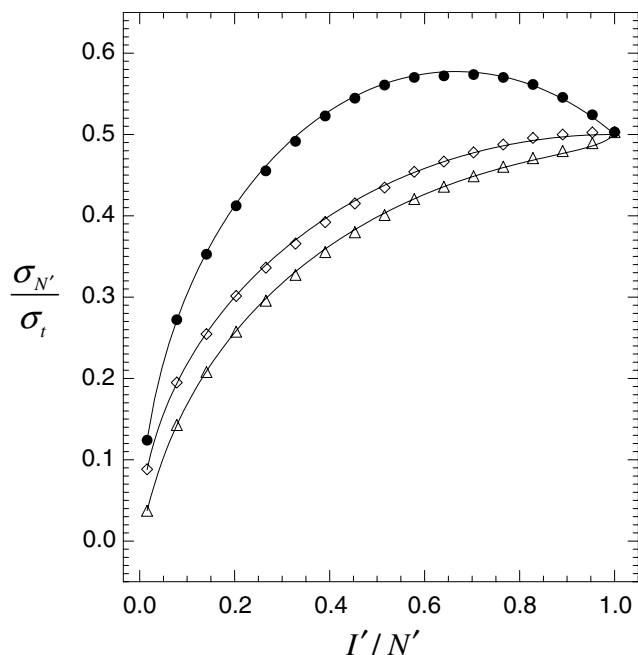


Fig. 1. Standard deviation of integrated noise,  $\sigma_{N'}$ , in units of the standard deviation of noise in the FID signal,  $\sigma_t$ , according to a Monte-Carlo simulation, plotted against the integrated fraction of the spectrum. Five thousand independent realizations of complex-valued Gaussian white noise (zero mean, standard deviation  $\sigma_t$ ) with  $N = 64$ , spectral width = 78 Hz, were processed: (i) without zero-filling ( $N' = N$ ) or apodization (full circles), (ii) with zero-filling only ( $N' = 2N$ ; open diamonds), and (iii) with zero-filling ( $N' = 2N$ ) and with exponential apodization ( $\alpha = 2.0$  Hz; open triangles). All simulations and calculations were carried out using IDL (Interactive Data Language, Research Systems Inc., Boulder, CO). Solid lines represent calculations according to: Eq. (17b) (i), Eq. (19) (ii), and Eqs. (7) and (12b) (iii).

simulation without apodization or time-domain signal shift. The result is plotted against the integrated fraction of the spectrum in each dimension,  $I'/N'$  and  $J'/N'$ . For simplicity, only rectangular integration intervals are considered. The calculations according to Eqs. (7) and (16b), represented by the black dashed lines in Fig. 5, rely on the fact that the Fourier transform of the two-dimensional time-domain signal can be separated into a product of two one-dimensional transforms [14]. Furthermore, the first point of each FID in each of the two dimensions is multiplied by 1/2 [17].

#### 4. Discussion

As mentioned earlier, the spectral interpolation effectively introduced by zero-filling, increases the information contained in each of the real and the imaginary part of the signal by the amount of additional information contained in the respective other part [1]. While a maximum sensitivity enhancement by a factor of  $\sqrt{2}$  is expected for  $N' = 2N$ , adding more zeroes to the time-domain signal does not lead to any further gain. Our results are in agreement with these statements. It was shown that for small integration intervals,  $I' \ll N'$ , and provided that no shift was applied to the time-domain signal prior to FT, the relation  $\sigma_{N'}/\sigma_N \rightarrow 1/\sqrt{2}$  holds. It can be shown that this corre-

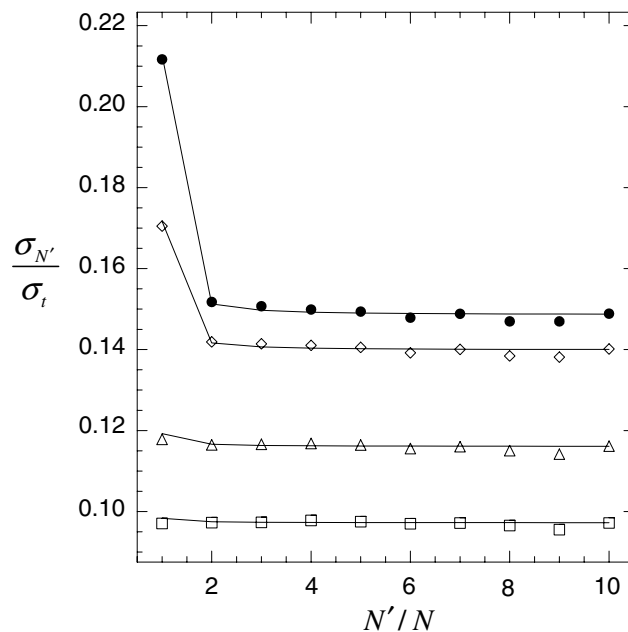


Fig. 2. Standard deviation of integrated noise,  $\sigma_{N'}$ , in units of the standard deviation of noise in the FID signal,  $\sigma_t$ , according to a Monte-Carlo simulation, plotted against the number of spectral points after zero-filling,  $N'$ , in units of  $N$  (see caption for Fig. 1 for more details on the simulation). Each integration was carried out over the equivalent of  $I = 3$  spectral points. Data shown are for: (i) no apodization (full circles), (ii) mild exponential apodization ( $\alpha = 0.2$  Hz, open diamonds), (iii) moderate exponential apodization ( $\alpha = 1.0$  Hz, open triangles), and (iv) strong exponential apodization ( $\alpha = 2.0$  Hz, open squares). Solid lines represent calculations according to Eqs. (7) and (16b) (i), and Eqs. (7) and (12b) ((ii)–(iv)).

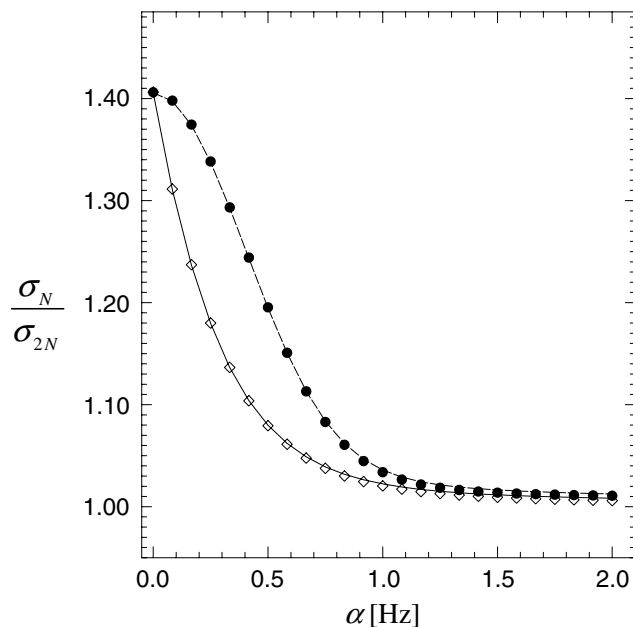


Fig. 3. Ratio of the standard deviation of integrated noise obtained for an FID signal without zero-filling versus zero-filling with  $N' = 2N$  according to a Monte-Carlo simulation, plotted against the strength of the apodization filter (see caption for Fig. 1 for more details on the simulation). Each integration was carried out over the equivalent of  $I = 3$  spectral points. Data shown are for: (i) exponential apodization (open diamonds), and (ii) Gaussian apodization (full circles). Lines represent calculations according to Eqs. (7) and (12b).

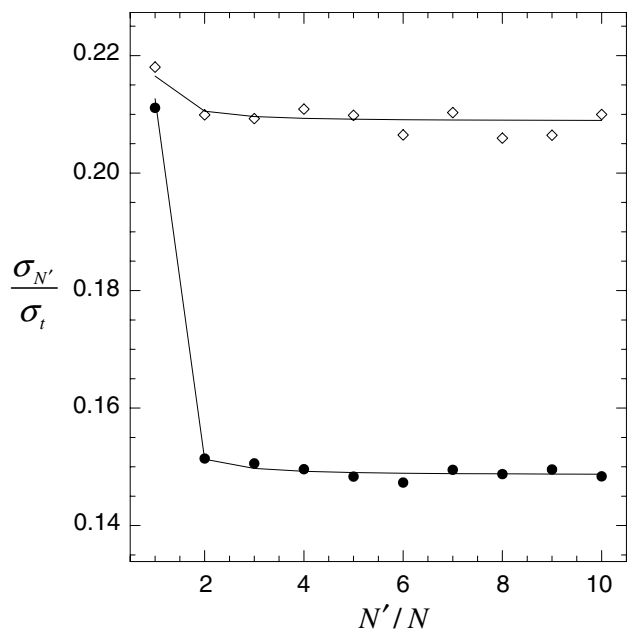


Fig. 4. Standard deviation of integrated noise in units of the standard deviation of noise in the time-domain signal according to a Monte-Carlo simulation, plotted against the number of spectral points after zero-filling,  $N'$ , in units of  $N$  (see caption for Fig. 1 for more details on the simulation). Each integration was carried out over the equivalent of  $I = 3$  spectral points, and no apodization was used. Data shown are for (i) no shift of the time-domain signal prior to FT (full circles), and (ii) a time shift of  $M = N/2$  (symmetric spin-echo; open diamonds). Solid lines represent calculations according to Eqs. (7) and (16b) (i), and Eqs. (7) and (16a) (ii).

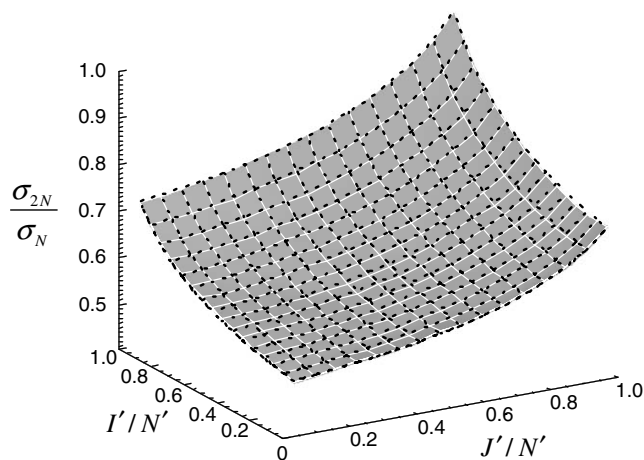


Fig. 5. Ratio of the standard deviation of integrated noise for zero-filling with  $N' = 2N$  versus no zero-filling according to a 2D NMR Monte-Carlo simulation (2D FID), plotted against the integration interval in each dimension (see caption for Fig. 1 for more details on the simulation). Prior to zero-filling, the two-dimensional matrix had dimensions  $N \times N = 16 \times 16$ . Ratios are plotted against the integrated fraction of the spectrum in each dimension,  $I'/N'$  and  $J'/N'$ . Simulated data are represented by white lines, while calculations according to Eqs. (7) and (16b) are represented by black dashed lines.

sponds to the maximum sensitivity enhancement achievable by zero-filling. For larger integration intervals, the ratio  $\sigma_{N'}/\sigma_N$  will be larger, approaching a value of 1 for  $I'$  and  $I$  approaching  $N'$  and  $N$ , respectively. This is based

on the fact that full spectral integration always yields  $\sigma_{N'}(I' = N') = \sigma_t$  (spin-echo) or  $\sigma_{N'}(I' = N') = \sigma_t/2$  (FID), regardless of the value of  $N'$ . Consequently, it may be advantageous to limit spectral integration to the smallest possible interval in order to preserve the sensitivity enhancement provided by zero-filling. As Figs. 2 and 4 demonstrate, zero-filling beyond  $N' = 2N$  does not lead to any further reduction in the standard deviation of the spectral integral, in agreement with [1]. In particular, without apodization or time shift, Eq. (19) describes the standard deviation of the spectral integral for any  $N' = nN$ , with<sup>3</sup>  $n \geq 2$ . As shown in Fig. 1 for the case of an FID signal, the standard deviation of the spectral integral increases with increasing integration interval until it reaches a local maximum, after which it falls towards the value of  $\sigma_t/2$  for integration of the full spectral width. For small integration intervals, all time-domain points contribute with nearly equal weights to the integral,<sup>4</sup> which explains the strong initial increase in  $\sigma_N$ . For larger integration intervals, the signal value at  $t = 0$  increasingly dominates the result, which reduces the increase in  $\sigma_N$ , and finally, for intervals close to the full spectral width,  $\sigma_N$  approaches  $\sigma_t/2$ . These observations are a direct result of the correlation between spectral points caused by the multiplication of the first point in the FID by  $1/2$ . It should be noted that without and with zero-filling, according to Eqs. (17b) and (19), respectively, the correlation tends to disappear for small integration intervals, as the approximations  $\sigma_N(I) \propto \sqrt{I}$  and  $\sigma_{2N}(I) \propto \sqrt{I}$  for  $I \ll N$  reveal.

Fig. 4 shows that application of a left-shift to the time-domain signal by  $M = N/2$  points after zero-filling but prior to FT causes zero-filling to be largely ineffective in reducing the standard deviation of the spectral integral. In practice, this shift would be applied to symmetrically acquired spin-echo signals with the additional zeroes introduced by zero-filling to the right of the measured  $N$  points. As is well known, the FT of the symmetric, noise-free spin-echo signal produces a spectrum whose imaginary part is exactly zero. The entire information is therefore contained in the real part. This is true with or without zero-filling. From this and the above discussion for the case of  $M = 0$  it could be assumed that zero-filling would have no effect on the standard deviation of the spectral integral. However, since the random nature of the noise effectively breaks the symmetry, a small effect is still obtained as shown in Fig. 4 for a small integration interval. Nevertheless, for all practical purposes, the effect of zero-filling can be neglected in the case of symmetric spin-echo signals.

Fig. 2 demonstrates the effect of exponential apodization on the standard deviation of the spectral integral. As expected, the standard deviation is reduced with increasing

<sup>3</sup> In general, however, it is not required that  $N'$  is an integer multiple of  $N$ .

<sup>4</sup> In fact, for  $I = 1$ , the integral corresponds to the direct sum of all time-domain points.

line broadening. Although it may seem possible that this reduction, in combination with zero-filling, could provide even higher sensitivity enhancement, this is, in fact, not the case. In Fig. 2, it can be seen that the reduction in the standard deviation due to zero-filling is also reduced as compared to processing without zero-filling. In particular, the difference in  $\sigma_{N'}/\sigma_I$  between  $N' = N$  and  $N' > N$  is decreasing with increasing strength of the apodization filter. This is shown in more detail in Fig. 3 for exponential and Gaussian apodization. Here the ratio  $\sigma_N/\sigma_{2N}$  is shown to decrease from its maximum value,  $\sqrt{2}$  (without apodization; see above), to values close to 1 for relatively moderate line broadening values. This behavior is due to the apodization filter imposing a correlation between the real and imaginary parts of the time-domain signal [1]. Thus, the two parts no longer contain independent information, and the transfer of information from one part into the other due to zero-filling described above becomes increasingly negligible.

Since the spatial dimensions in MRSI are usually sampled on a symmetric grid around the center of k-space and FT is used for spatial reconstruction [21–23], the above discussion of zero-filling for symmetric spin-echo signals indicates that zero-filling will have a negligible effect on spatial integrals (voxel averages). If the time-dimension is sampled from an FID signal, zero-filling in this dimension will, of course, still have the same effect on the standard deviation of spectral integrals described above.

The result shown in Fig. 5 demonstrates that the results presented in this communication for one-dimensional signals can be extended to multiple dimensions in a straightforward manner. Note that complex-valued spectral data was considered. While magnitude-mode spectral 2D data, 1D cross-sections, or projections onto a one-dimensional axis are often used in the analysis of 2D NMR data, complex-valued data was used here for illustration purposes. Since the noise behavior will depend on the axis chosen for cross-section or projection, and since the noise distribution in magnitude data depends on the signal intensity [24], a general analysis of the standard deviation of integrals of 2D spectral data is difficult. The same is true for integrals calculated for arbitrarily shaped integration regions, which is why only rectangular integration regions are considered here. The integral over the entire spectral data (data not shown) yields  $\sigma_{N',N'} = \sigma_I/4$  [14], regardless of the value of  $N'$ , which again reflects the fact that the full integral of the spectral signal equals the value of the time-domain signal at time  $t_1 = 0$  and  $t_2 = 0$ . At the other extreme, when integration is limited to very small regions, Fig. 5 shows that  $\sigma_{N',N'}/\sigma_{N,N} \rightarrow 1/2$ , consistent with the fact that the two dimensions provide independent information such that each of them contributes a factor  $1/\sqrt{2}$ .

The majority of studies that examined the properties of integrals obtained from FT spectroscopic data treated either the time-domain signal [8,10] or both the time-domain signal and the frequency-domain signal as continu-

ously sampled [13,14]. This approach fails to account for zero-filling applied in the time-domain and the influence it has on how noise is propagated into spectral integrals. In the worst case, this approach can lead to the incorrect conclusion that zero-filling is of no consequence for spectral integration [13]. In addition, in most of these studies, simulations to validate expressions were absent, and if they were conducted, zero-filling was excluded a priori [13]. Previously, Bourg and Nuzillard presented an analysis that accounted for the discrete nature of NMR data [15]. However, simulations were again missing, and neither time shifts nor the multiplication of the first point of an FID by 1/2 was accounted for in their approach. Furthermore, several expressions derived in that work described the standard deviation of spectral integrals incorrectly. For example, Eq. (12) in [15], on which Eqs. (15) and (17) in [15] are based, states that in the absence of apodization  $\sigma_I^2 = \sigma_F^2 \sum_{k=0}^{n-1} [\sin(km\pi/N)/\sin(k\pi/N)]^2$ , where  $\sigma_I$  is the standard deviation of the spectral integral carried out over  $m$  points, and  $\sigma_F$  is the mean standard deviation of the time-domain signal consisting of  $n$  sampling points, and zero-filled to  $N$  points. If the entire spectral range were to be integrated, i.e., if  $m = N$ , only the term with  $k = 0$  would remain in the sum with a value of 1, and  $\sigma_I = \sigma_F$ . However, the authors state that, in their own notation, this result is expected to be  $\sigma_I = n \cdot \sigma_F$ .

## 5. Conclusions

This communication provides expressions allowing the calculation of the standard deviation of spectral integrals obtained from the Fourier-transform of discretely sampled data as a function of zero-filling and/or apodization applied and as a function of the integration interval. The expressions derived were validated using Monte-Carlo simulations, and a few approximations of practical importance were presented. Our results are in agreement with the basic findings in the seminal work by Bartholdi and Ernst [1] but provide information that goes beyond more recently published studies. It was demonstrated that apodization tends to alleviate the reduction in standard deviation of spectral integrals obtained by zero-filling. Even though, for mild apodization, some beneficial effect may be preserved, stronger apodization filters that are often encountered in practice can obliterate it completely. Furthermore, the time shift applied to symmetric spin-echo signals reduces the beneficial effect of zero-filling to a negligible level. Voxel averaging in multi-dimensional spectroscopic imaging methods that use symmetric sampling of k-space will therefore not benefit from zero-filling in k-space. A similar conclusion can be drawn for voxel averaging in many MRI methods. Results for 2D NMR indicate that the calculations presented for 1D signals are readily expanded for multi-dimensional data, although details of the data processing can complicate the analysis. It was furthermore shown that the analysis of the standard deviation of spectral integrals amounts to

an analysis of correlation among the spectral points contributing to the integral. In particular, it was demonstrated that multiplication of the first point in the FID signal by a factor 1/2 causes a correlation among spectral intensities. In addition, while in the absence of this multiplication and without zero-filling or apodization, spectral intensities remain uncorrelated, both procedures introduce a correlation affecting the standard deviation of spectral integrals as a function of the length of the integration interval. In order to achieve best results, i.e., maximum SNR enhancement as compared to data processed without zero-filling, it is advantageous to limit the size of the integration interval.

### Acknowledgment

Support from the VA Medical Center San Francisco is gratefully acknowledged.

### Appendix A. Derivation of Eqs. (16a) and (16b)

In the absence of apodization, the inner sum in Eq. (11a), defined by  $C := \sum_{j=0}^{N-1} (q_-^{j-M} + q_+^{j-M})$ , can be evaluated as follows:

$$C_d = p_+ \sum_{j=0}^{N-1} q_-^j + p_- \sum_{j=0}^{N-1} q_+^j \quad \text{with } p_{\pm} := q_{\mp}^{-M}.$$

Evaluation of the geometric sums leads to

$$\begin{aligned} C_d &= p_+ \frac{1 - q_-^N}{1 - q_-} + p_- \frac{1 - q_+^N}{1 - q_+} = p_+ \frac{1 - q_-^N}{1 - q_-} - p_- \frac{q_- - q_+^{N-1}}{1 - q_-} \\ &= \frac{p_+ - p_- q_- - p_+ q_-^N + p_- q_+^{N-1}}{1 - q_-} \\ &= \frac{p_+ q_-^{-1/2} - p_- q_-^{+1/2}}{q_-^{-1/2} - q_-^{+1/2}} + \frac{p_- q_-^{-N+1/2} - p_+ q_-^{N-1/2}}{q_-^{-1/2} - q_-^{+1/2}}. \end{aligned}$$

Note that  $q_+ = 1/q_-$ . Substituting  $q_{\pm} = \exp(\pm 2\pi id/N')$  and  $p$  by the corresponding complex exponential functions yields:

$$\begin{aligned} C_d &= \frac{\exp[\pi id(1 + 2M)/N'] - \exp[-\pi id(1 + 2M)/N']}{\exp(\pi id/N') - \exp(-\pi id/N')} \\ &\quad + \frac{\exp[2\pi id(N - \frac{1}{2} - M)/N'] - \exp[-2\pi id(N - \frac{1}{2} - M)/N']}{\exp(\pi id/N') - \exp(-\pi id/N')} \\ &= \frac{\sin[\pi d(1 + 2M)/N'] + \sin[2\pi d(N - \frac{1}{2} - M)/N']}{\sin(\pi d/N')}. \end{aligned}$$

Substitution of the inner sum in Eq. (11a) by this result for  $C_d$  (and observing that  $A = N$ ) leads to Eq. (16a). The inner sum in Eq. (11b),  $C'_d := \sum_{j=1}^{N-1} (q_-^j + q_+^j) = \sum_{j=0}^{N-1} (q_-^j + q_+^j) - 2$ , can be evaluated in a similar way yielding

$$C'_d = \frac{\sin[2\pi d(N - \frac{1}{2})/N']}{\sin(\pi d/N')} - 1.$$

Using this result in the evaluation of the inner sum in Eq. (11b), i.e.,  $\sum_{d=1}^{I'-1} (I' - 1)C'_d$ , yields Eq. (16b) after some basic transformations.

### Appendix B. Derivation of Eq. (18)

In the absence of apodization, and time shift, and for zero-filling  $N' = 2N$ , the trigonometric term in Eq. (16b) defined as  $D_d := \sin[2\pi d(N - 1/2)/N']/\sin(\pi d/N')$  can be rewritten as follows:

$$\begin{aligned} D_d &= \frac{\sin(x - y)}{\sin y} \\ &= \frac{\sin x \cos y - \cos x \sin y}{\sin y}, \quad \text{with the definitions} \end{aligned}$$

$$x := \frac{2\pi dN}{N'} = \pi d \quad \text{and} \quad y := \frac{\pi d}{N'} = \frac{\pi d}{2N}.$$

Observing that

$$\cos x = \begin{cases} +1 & \text{for even } d \\ -1 & \text{otherwise} \end{cases}, \quad \text{and} \quad \sin x = 0 \quad \text{for all } d,$$

it follows that

$$D_d = \begin{cases} -1 & \text{for even } d \\ +1 & \text{otherwise.} \end{cases}$$

Therefore, we obtain for the sum in Eq. (16b):

$$\begin{aligned} E &:= \sum_{d=1}^{I'-1} [(I' - d)D_d] = \sum_{d=1}^{2I-1} [(2I - d)D_d] \\ &= \sum_{m=1}^I \{ [2I - (2m - 1)]D_{2m-1} \} + \sum_{n=1}^{I-1} [(2I - 2n)D_{2n}] \\ &= \sum_{m=1}^I [2I - (2m - 1)] - \sum_{n=1}^{I-1} (2I - 2n) \\ &= \sum_{m=1}^I 1 = I. \end{aligned}$$

Substitution of this result into Eq. (16b) immediately yields Eq. (18).

### References

- [1] E. Bartholdi, R.R. Ernst, Fourier spectroscopy and the causality principle, *J. Magn. Reson.* 11 (1973) 9–19.
- [2] J.C. Lindon, A.G. Ferrige, Digitisation and data processing in Fourier transform NMR, *Prog. NMR Spectrosc.* 14 (1980) 27–66.
- [3] C. Zwingmann, D. Leibfritz, A.S. Hazell, Brain energy metabolism in a sub-acute rat model of manganese neurotoxicity: an ex vivo nuclear magnetic resonance study using  $[1-^{13}\text{C}]$  glucose, *Neurotoxicology* 25 (2004) 573–587.
- [4] P.-G. Henry, Ö. Gülin, S. Provencher, R. Gruetter, Toward dynamic isotopomer analysis in the rat brain in vivo: automatic quantitation of  $^{13}\text{C}$  NMR spectra using LCModel, *NMR Biomed.* 16 (2003) 400–412.
- [5] X. Golay, J. Gillen, P.C. van Zijl, P.B. Barker, Scan time reduction in proton magnetic resonance spectroscopic imaging of the human brain, *Magn. Reson. Med.* 47 (2002) 384–387.
- [6] A. Gambini, S.A. Fatemi, T.O. Crawford, E.H. Kossoff, A. Horska, P.B. Barker, Acute disseminated encephalomyelitis: evaluation with

- proton MR spectroscopic imaging. In: Proc. 13th Annual Meeting of ISMRM, Miami Beach, FL, 2005, p. 140.
- [7] M.A. Thomas, N. Hattori, M. Umeda, T. Sawada, S. Naruse, Evaluation of two-dimensional L-COSY and JPRESS using a 3 T MRI scanner: from phantoms to human brain in vivo, *NMR Biomed.* 16 (2003) 245–251.
- [8] G.H. Weiss, J.A. Ferretti, Accuracy and precision in the estimation of peak areas and NOE factors, *J. Magn. Reson.* 55 (1983) 397–407.
- [9] F.G. Herring, P.S. Phillips, Integration errors in digitized magnetic resonance spectra, *J. Magn. Reson.* 62 (1985) 19–28.
- [10] G.H. Weiss, J.A. Ferretti, R.A. Byrd, Accuracy and precision in the estimation of peak areas and NOE factors. II. the effects of apodization, *J. Magn. Reson.* 71 (1987) 97–105.
- [11] K. McLeod, M.B. Comisarow, Systematic errors in the discrete integration of FT NMR spectra, *J. Magn. Reson.* 84 (1989) 490–500.
- [12] C. Rischel, Fundamentals of peak integration, *J. Magn. Reson. A* 116 (1995) 139–280.
- [13] R. Nadjari, J.-P. Grivet, Precision of integrals in quantitative NMR, *J. Magn. Reson.* 91 (1991) 353–361.
- [14] R. Nadjari, J.-P. Grivet, Precision of volume integrals in two-dimensional NMR, *J. Magn. Reson.* 98 (1992) 259–270.
- [15] S. Bourg, J.M. Nuzillard, Influence of noise on peak integrals obtained by direct summation, *J. Magn. Reson.* 134 (1998) 184–188.
- [16] A. Ebel, Schnelle <sup>1</sup>H NMR-spektroskopische Bildgebung mittels angepaßter Phasenkodierung der chemischen Verschiebung (Ph.D. thesis), University of Bremen, Bremen, and Shaker Verlag GmbH, Aachen, 1999.
- [17] G. Otting, H. Widmer, G. Wagner, K. Wüthrich, Origin of t1 and t2 ridges in 2D NMR spectra and procedures for suppression, *J. Magn. Reson.* 66 (1986) 187–193.
- [18] R. Durrett, *Probability: Theory and Examples*, Duxbury Press, Belmont, CA, 1991.
- [19] R.R. Ernst, Sensitivity enhancement in magnetic resonance. I. Analysis of the method of time averaging, *Rev. Sci. Instr.* 36 (1965) 1689–1695.
- [20] E.M. Haacke, R. Brown, M. Thompson, R. Venkatesan, *Magnetic Resonance Imaging - Physical Principles and Sequence Design*, Wiley-Liss (John Wiley & Sons), New York, NY, 1999.
- [21] A.A. Maudsley, G.B. Matson, J.W. Hugg, M.W. Weiner, Reduced phase encoding in spectroscopic imaging, *Magn. Reson. Med.* 31 (1994) 645–651.
- [22] J.W. Hugg, A.A. Maudsley, M.W. Weiner, Comparison of k-space sampling schemes for multidimensional MR spectroscopic imaging, *Magn. Reson. Med.* 36 (1996) 469–473.
- [23] E. Adalsteinsson, P. Irarrazabal, S. Topp, C. Meyer, A. Macovski, D.M. Spielman, Volumetric spectroscopic imaging with spiral based k-space trajectories, *Magn. Reson. Med.* 39 (1998) 889–898.
- [24] Z. Liang, A.G. Marshall, Time-domain (interferogram) and frequency-domain (absorption-mode and magnitude-mode) noise and precision in Fourier transform spectrometry, *Appl. Spectrosc.* 44 (1990) 766–775.